Optical helicity of unpolarized light

Kayn A. Forbes

School of Chemistry, University of East Anglia, Norwich, NR4 7TJ, U.K.

k.forbes@uea.ac.uk

Like energy and momentum, optical helicity is a fundamental dynamical property of light. In the prevalent plane wave and paraxial description of light the optical helicity is directly proportional to the degree of circular polarization, being zero for both linearly and unpolarized fields. Here it is shown that the non-paraxial fields generated by tightly focused optical vortices which have the phase factor $\exp(i\ell\phi)$ possess a contribution to the optical helicity density that is completely independent of the polarization state of the source paraxial field. In stark contrast to what is known in classical optics with plane waves and paraxial light, the physical consequence is that unpolarized light can exhibit optical activity and chiral light-matter interactions.

Non-paraxial optical fields exhibit fascinating properties compared to the plane waves and paraxial fields which have dominated classical optics and light-matter interactions for decades. In recent years, with the growth of modern nano-optics and photonics, the extraordinary properties of non-paraxial fields have found widespread utilization [1,2]. In this work we refer to paraxial modes and propagating plane waves as two-dimensional (2D) structured fields, in that they may possess inhomogeneous spatial or polarization degrees of freedom in the transverse (x,y) plane, but are homogenous in the direction of propagation (z) [3]. Such 2D structured fields are also usually examined in terms of their 2D polarization states. Three-dimensional (3D) structured optical fields are inhomogeneous along their direction of propagation, examples include evanescent waves or tightly focussed laser beams, the essential requirement being electromagnetic fields that are spatially confined in some way or another. A crucial difference between 2D and 3D structured light is that in addition to the usually dominant transverse fields, the latter possess significant longitudinal components of their electromagnetic fields with respect to the direction of propagation. The non-paraxial nature and 3D structure of spatially confined optical fields has led to some remarkable light-matter interactions [4–7], which are especially striking when compared to the prevailing textbook description of light-matter interactions in terms of propagating plane waves. Because all three spatial components of the field vector generally play a role in non-paraxial light, the theory of polarization has been extended to the 3D case [8–10]. While generic 2D polarization is described by four Stokes parameters, 3D polarization is characterized by nine polarization parameters. Crucially, a totally unpolarized 2D field is at least half-polarized in the 3D sense [11,12], and for tightly focused unpolarized paraxial beams it has been demonstrated that the focused field produces rings of light which are locally fully polarized in a 3D sense [13,14].

One of the extraordinary properties of non-paraxial optical fields is that they possess a transverse spin momentum, orthogonal to the main direction of propagation [15–18]. Eismann, et al. [12] have recently proven both theoretically and experimentally that this transverse spin momentum is largely independent of 2D polarization, and remarkably survives in 3D fields generated from a 2D unpolarized optical source. This is in sharp contrast to longitudinal spin which is directly related to 2D polarization. Subsequently, Chen et al. [19] extended the theory to account for the electric field component of the spin for focused random light of arbitrary degree of polarization. Related to spin angular momentum is the optical helicity, and in fact both are correlated to one another by a continuity equation [20–23]. However, both contribute to experimentally distinct observables, with spin producing mechanical spinning motions of probe particles [15–17] while optical helicity is proportional to the optical chirality for monochromatic fields and is responsible for optical activity and chiral light-matter interactions [24–31]. In the plane wave case, it is well known that optical helicity is proportional to the degree of 2D circular polarization: it is zero for 2D linearly polarized or 2D unpolarized optical fields and takes on its maximum value for 2D circular polarization. Here we show that 3D structured light beams generated from a 2D source which possesses the azimuthal phase factor $\exp(i\ell\phi)$, commonly referred to as optical vortices or twisted light [32], acquire a non-zero contribution to the optical helicity density that is fully independent of the 2D polarization state, being generated even by a 2D unpolarized optical vortex light source. The striking physical consequence of this is that light generated from totally unpolarized paraxial light can exhibit optical activity.

Optical helicity $\mathcal{H}$ in the Coulomb gauge is defined as [20,22,28]

$$\mathcal{H} = \int d^3\boldsymbol{r}\,\frac{\varepsilon_0 c}{2}\left(\boldsymbol{A}^{\perp}\cdot\boldsymbol{B} - \boldsymbol{C}^{\perp}\cdot\boldsymbol{E}\right), \tag{1}$$

where $\boldsymbol{A}^{\perp}$ $\boldsymbol{C}^{\perp}$ are the vector potentials and $\boldsymbol{E}$ $\boldsymbol{B}$ the electric and magnetic field, respectively. The vector potentials and electromagnetic fields are related to one another as [20,22] $\boldsymbol{E}=-\nabla\times\boldsymbol{C}^{\perp}=-\dot{\boldsymbol{A}}^{\perp}$ and $\boldsymbol{B}=\nabla\times\boldsymbol{A}^{\perp}=-\dot{\boldsymbol{C}}^{\perp}$. The total helicity $\mathcal{H}$ (1) is both gauge and Lorentz invariant, however the integrand, which represents the optical helicity density h, is not Lorentz invariant. Lorentz invariance is sacrificed to make h gauge invariant, important for calculating experimentally determinable physical quantities in optics [23]. Noting that for monochromatic fields [22] $i\omega\boldsymbol{A}^{\perp}=\boldsymbol{E}$ and $i\omega\boldsymbol{C}^{\perp}=\boldsymbol{B}$, the cycle-averaged helicity density $\bar{h}$ for classical fields is [22]

$$\bar{h}=-\frac{\varepsilon_0 c}{2\omega}\operatorname{Im}\left(\boldsymbol{E}^{*}\cdot\boldsymbol{B}\right). \tag{2}$$

Clearly both expressions (1)-(2) are conserved quantities of the field, i.e. $\dot{\mathcal{H}},\dot{h},\dot{\bar{h}}=0$. For 2D structured light, propagating plane waves, and even evanescent waves the optical helicity is directly proportional to the degree of circular polarization $\bar{h}\propto\sigma$, where $\sigma=\pm1$ for circularly polarized light and is zero for both linearly and unpolarized light [4].

In this work we are mainly interested in calculating $\bar{h}$ for 3D structured Laguerre-Gaussian (LG) modes generated from a 2D unpolarized source. The simplest way to calculate this is to average the conserved quantity over two orthogonal 2D polarization states on the Poincaré sphere. We therefore choose to average over two electric fields, one linearly polarized in the *x* direction and the other in the *y* direction (with the corresponding magnetic fields polarized in the *y* and -*x* directions, respectively).

The electric field for a 2D-*x* polarized monochromatic 3D LG mode in the first post-paraxial approximation is [33,34]

$$\boldsymbol{E}_{\mathrm{LG}}=E_0\left\{\hat{\boldsymbol{x}}+\hat{\boldsymbol{z}}\frac{i}{k}\left(\gamma\cos\phi-\frac{i\ell}{r}\sin\phi\right)\right\}u_{\ell,p}^{\mathrm{LG}}\left(r,\phi,z\right), \tag{3}$$

where E_0 is the field amplitude, $\gamma=\left\{\frac{|\ell|}{r}-\frac{2r}{w^2(z)}+\frac{ikr}{R(z)}-\frac{4r}{w^2(z)}\frac{L_{p-1}^{|\ell|+1}}{L_p^{|\ell|}}\right\}$, and $u_{\ell,p}^{\mathrm{LG}}\left(r,\phi,z\right)$ is [35,36]

$$u_{\ell,p}^{\mathrm{LG}}\left(r,\phi,z\right)\sqrt{\frac{2p!}{\pi w_0^2\left(p+|\ell|!\right)}}\frac{w_0}{w(z)}\left(\frac{\sqrt{2}r}{w(z)}\right)^{|\ell|}L_p^{|\ell|}\left[\frac{2r^2}{w^2(z)}\right]\exp\left(-r^2/w^2(z)\right)$$
$$\exp i\left(kz+\ell\phi-\omega t+kr^2/2R(z)-(2p+|\ell|+1)\xi(z)\right), \tag{4}$$

$\ell \in \mathbb{Z}$ is the pseudoscalar topological charge; p is the radial index, all other quantities have their usual meanings. The $\hat{\boldsymbol{x}}$ dependent term in (3) is the transverse field component and taken alone represents a 2D structured and polarized LG mode; the $\hat{\boldsymbol{z}}$ dependent term is the longitudinal field, responsible for 3D structure. The magnitude of the longitudinal component is proportional to λ / w_0, i.e. the ratio of the input wavelength to the beam waist, becoming larger the more tightly focused the field is. The corresponding magnetic field is given by

$$\boldsymbol{B}_{\mathrm{LG}} = B_0 \left\{ \hat{\boldsymbol{y}} + \hat{\boldsymbol{z}} \frac{i}{k} \left(\gamma \sin\phi + \frac{i\ell}{r} \cos\phi \right) \right\} u_{\ell,p}^{\mathrm{LG}}(r,\phi,z). \tag{5}$$

Inserting (3) and (5) into (2) gives the optical helicity density as

$$\bar{h}^{x} = -\mathrm{Re} \frac{I(r,z)}{c\omega} \frac{\ell}{k^2 r} \gamma, \tag{6}$$

where $I(r,z) = \frac{c\varepsilon_0}{2} E_0^2 \left| u_{\ell,p}^{\mathrm{LG}} \right|^2$ is the input beam intensity. It is crucial to realize that this optical helicity density stems purely from the longitudinal field components and so is not exhibited by 2D structured light. It is proportional to ℓ, and so is unique to 3D structured beams that possess an azimuthal phase $\exp(i\ell\phi)$. Optical helicity of a 2D structured field comes purely from the degree of 2D circular polarization of the transverse fields.

For the orthogonally polarized beam the electric and magnetic fields are

$$\boldsymbol{E}_{\mathrm{LG}} = E_0 \left\{ \hat{\boldsymbol{y}} + \hat{\boldsymbol{z}} \frac{i}{k} \left(\gamma \sin\phi + \frac{i\ell}{r} \cos\phi \right) \right\} u_{\ell,p}^{\mathrm{LG}}(r,\phi,z), \tag{7}$$

$$\boldsymbol{B}_{\mathrm{LG}} = B_0 \left\{ -\hat{\boldsymbol{x}} - \hat{\boldsymbol{z}} \frac{i}{k} \left(\gamma \cos\phi - \frac{i\ell}{r} \sin\phi \right) \right\} u_{\ell,p}^{\mathrm{LG}}(r,\phi,z). \tag{8}$$

Inserting (7) and (8) into (2) gives

$$\bar{h}^{y} = -\mathrm{Re} \frac{I(r,z)}{c\omega} \frac{\ell}{k^2 r} \gamma, \tag{9}$$

and for unpolarized (n) light the optical helicity density $\bar{h}^{n}$ is therefore

$$\bar{h}^{n} = \frac{\bar{h}^{x} + \bar{h}^{y}}{2} = \bar{h}^{x}. \tag{10}$$

This optical helicity density is fully independent of the 2D polarization of the transverse field. For example, taking a paraxial 2D structured vortex and tightly focusing it to create a 3D structure, the ensuing optical helicity density contribution (10) generated is completely independent of the 2D polarization state of the input paraxial structured mode. The 2D polarization independent optical helicity density (10) is plotted in Figure 1 at w_0. The focal plane is concentrated upon because helicity in the far field is purely a measure of 2D circular polarization [37]. For cases where $p=0$ we produce two distinct rings of helicity density with different signs, and in the case of $|\ell|=1$ we produce an on-axis helicity density. The magnitude of the optical helicity density in the outer ring is smaller than the inner ring and of the opposite sign. Small probe chiral particles and nanostructures in the focal region will experience differential light-matter interactions depending on their position in the transverse plane and their handedness. For example, comparison of Figure 1a and 1b shows that a chiral particle of a given handedness positioned in the centre of the focal spot of a tightly focused 2D unpolarized LG $(|\ell|=1, p=0)$ beam will absorb or scatter the $\ell=1$ at a different rate to the $\ell=-1$ source beam. The case of $p=0$ has been concentrated on in Figure 1 because of the fact this is the radial index predominantly implemented in experiments involving LG beams. However, (10) is general and applies to any mode (ℓ, p). Increasing p has two effects: firstly, $(2p+2)$ rings of helicity density are produced in general and secondly, we increase the relative magnitude of the longitudinal fields responsible for the 2D-polarization independent helicity density because increasing p leads to larger transverse field gradients and thus larger longitudinal field components.

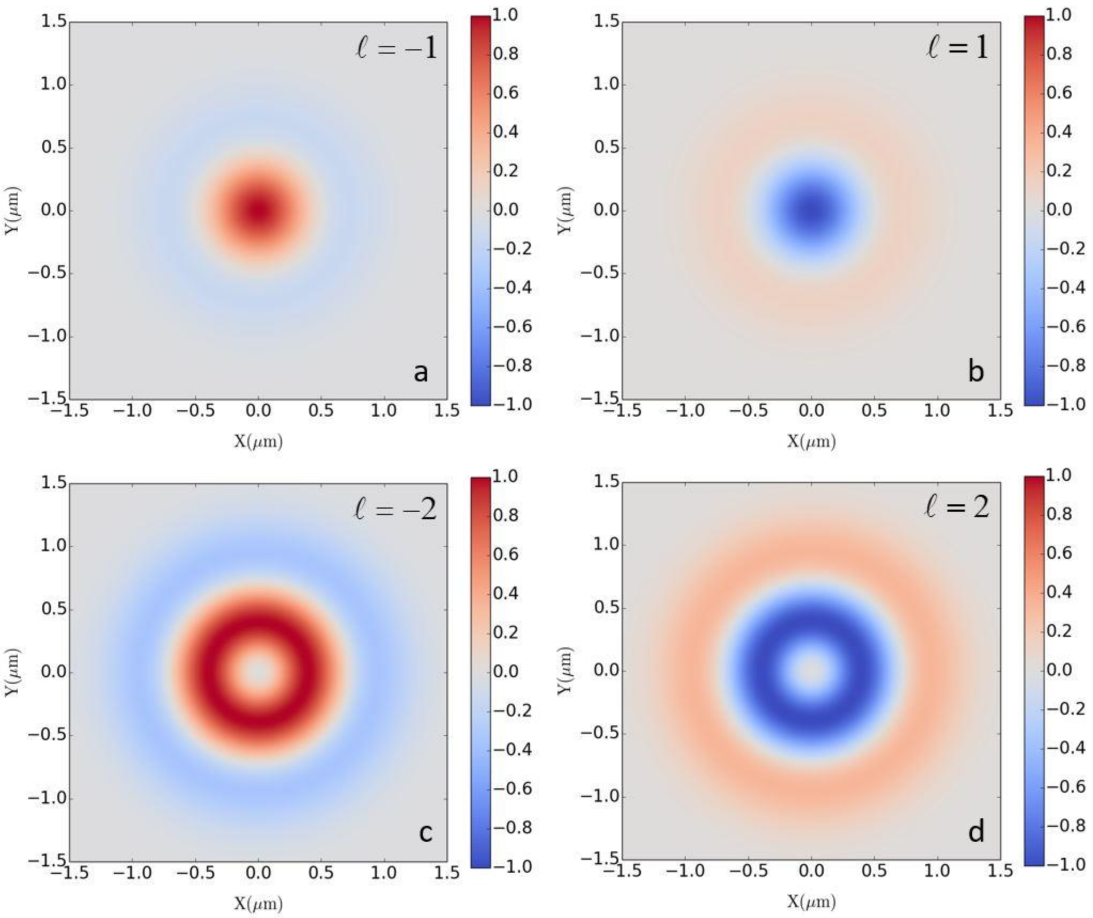

Figure 1: normalized 2D polarization independent optical helicity density (10) at $w_0\left(z=0\right)$. $p=0$ in (a)-(d).

It is important to note that this 2D polarization independent contribution to the optical helicity density we are concerned with does not contribute to the integrated value of optical helicity:

$$\mathcal{H}=\int \bar{h}d^2\boldsymbol{r}=0. \tag{11}$$

Its experimental observation therefore requires particles smaller than the transverse dimension of the focal field.

It must be emphasized that this 2D polarization independent contribution to the optical helicity density is proportional to ℓ and so linearly/randomly polarized Gaussian or Hermite-Gaussian beams, for example, do not possess it regardless of whether they are 2D or 3D structured. The input 2D beam must possess the phase factor $\exp\left(i\ell\phi\right)$, so Bessel beams, for example, would also display this 2D polarization independent optical helicity density contribution. The reason for this is that the origin of the longitudinal fields of 3D modes which generate this 2D polarization independent optical helicity density are in the gradients of the transverse fields, i.e. $\propto \partial_r + \partial_\phi$, and it is the azimuthal gradient which provides the unique ℓ-dependent longitudinal component.

Our result for a 2D unpolarized 3D LG beam can be derived via an alternative method. The optical helicity density generated for a 3D field generated from a 2D circularly polarized paraxial LG mode is [34]

$$\bar{h}^{\sigma} = \frac{I(r,z)}{c\omega}\left(\sigma + \frac{1}{2k^2}\left[\sigma(\mathrm{Re}\,\gamma)^2 - \frac{2\ell}{r}\mathrm{Re}\,\gamma + \frac{\ell^2\sigma}{r^2}\right]\right), \tag{12}$$

where $\sigma = \pm 1$, the positive sign corresponding to a left-handed input and the negative sign right-handed. Adding the optical helicity densities calculated for the orthogonal polarizations $\sigma = 1$ and $\sigma = -1$ together and averaging the result gives the 2D unpolarized result:

$$\bar{h}^{n} = \frac{\bar{h}^{|\sigma|} + \bar{h}^{-|\sigma|}}{2} = -\mathrm{Re}\frac{I(r,z)}{c\omega}\frac{\ell}{k^2 r}\gamma, \tag{13}$$

which gives the identical optical helicity contribution as the method of averaging the optical helicity densities of two orthogonal linear polarizations (10). This alternative method of calculation equally proves that there is an optical helicity density which is 2D polarization independent in 3D vortex beams. It is also important to highlight that the middle term in square brackets in (12) is the 2D polarization independent optical helicity density term (i.e. (6), (9), (10), and (13)) and so we may also conclude that even when the input source field is 2D circularly polarized this 2D polarization independent contribution survives and is therefore robust again spin-orbit-interactions of light [5].

As mentioned above, recently it was theoretically and experimentally shown that transverse spin angular momentum is largely independent of the polarization state of the input 2D field in both focussed light and evanescent waves [12]. In their work the authors make the comment that ‘However, in our case of an unpolarized source, the helicity and longitudinal spin vanish.’ We are able to directly compare our results here to those in [12]. The fundamental Gaussian mode is simply LG_{00} and $\ell = 0$ in (13) shows that for a Gaussian beam $\bar{h}^{n} = 0$ in agreement with [12]. The input 2D field which generates the 3D Gaussian field and evanescent wave in [12] responsible for the 2D polarization independent transverse spin and zero helicity density does not possess the phase factor $\exp(i\ell\phi)$. An alternative physical interpretation to that given below (10) is that this azimuthal phase leads to the canonical momentum density having an azimuthal component, which when projected onto the 2D polarization independent (in the dual symmetric sense, see below) transverse spin angular momentum density leads to a non-zero helicity density for unpolarized light as we have shown here. In the case of a Gaussian beam [4] or evanescent wave [38] the canonical momentum density is purely in the longitudinal direction, and so even though these optical fields may possess a transverse spin density when generated from an unpolarized source, its projection on their canonical momentum density to yield the helicity gives zero in any circumstances.

Another point worth comparing between optical helicity density and transverse spin momentum density is that in [12] it is stated that the transverse spin angular momentum is 'largely independent of the polarization state'. The dual symmetric transverse spin $\boldsymbol{s}_{\perp} = \boldsymbol{s}_{\perp}^{E} + \boldsymbol{s}_{\perp}^{B}$ is fully independent of the polarization state, but the corresponding electric and magnetic spatial distributions do depend on the input 2D polarization, and this has important consequences in experimental observations due to the electric-bias nature of most materials (see *Appendix*). However, the optical helicity density contribution studied in this work is fully independent of 2D polarization in every respect, including its interaction with matter. The electric-magnetic asymmetry of matter does not influence optical helicity because by its very nature it couples to the interferences between electric and magnetic dipoles of chiral matter. This agrees with the fact that the dual symmetric and dual asymmetric optical helicities are identical [22,34].

In this work we have highlighted a contribution to the optical helicity density for 3D vortex beams which is fully independent of the 2D polarization state of the source, surviving even when the source is 2D unpolarized, and that its generation requires the incident optical field to possess the phase factor $\exp(i\ell\phi)$. The input 2D fields with this phase structure before spatial confinement possess zero optical helicity but they are geometrically chiral, i.e. they possess a non-zero Kelvin's chirality [39]. In contrast, the Kelvin's chirality of an unpolarized 2D Gaussian beam or propagating plane wave is zero. As such, it is only optical fields which possess a non-zero Kelvin's chirality which have the capacity to generate the 2D polarization independent optical helicity density contribution. Interestingly Kelvin's chirality does not interact (in a non-mechanical, spectroscopic sense) with chiral matter in the dipole approximation; multipole couplings of electric quadrupole nature or higher are required [40]. However, the 2D polarization independent optical helicity density contribution generated by these beams with Kelvin's chirality does interact via the interferences of electric and magnetic dipoles [37,41,42]. Is it therefore legitimate to suggest that there is a relationship between

Kelvin's chirality and optical helicity, and in certain scenarios the two become coupled? This is what Nechayev et al. [39] propose. The problem is that just like geometrical chirality of matter, there is seemingly no satisfactory way to quantify the scale-dependent Kelvin's chirality, and fundamentally there is of course no quantum operator for chirality.

Observation of an optical property necessarily requires a suitable light-matter interaction. Experimental observation of the 2D polarization independent contribution to the optical helicity density would be straightforward in this regard. For example, the experimental set up in Ref. [42] could very easily be modified to prove that 3D optical vortices possess a 2D polarization independent optical helicity density contribution by simply comparing the transmission of 2D unpolarized LG modes of $\ell = \pm 1, p = 0$ to that of any polarized Gaussian mode. Essential in any general experimental setup aiming to observe the 2D polarization independent optical helicity density of 3D vortex beams would be a tight focus using a high NA lens and chiral particles smaller than the transverse dimension w_0. Beyond these general considerations the signal magnitude of any given light-matter interaction depends on the material properties (i.e. molecular, plasmonic, etc.) and the fundamental interaction itself. It is known that a number of light-matter interactions are proportional to the optical helicity density [43], such as chiral optical forces, Rayleigh and Raman optical activity, and vortex dichroism [44], all of which provide a means to observe optical activity with unpolarized light, something which could never be envisaged with plane wave or paraxial light sources. This work therefore adds to the rapidly growing field of structured light and chirality [41].

This work has revealed a further fascinating property of optical vortices in that when tightly focused they acquire an optical helicity density contribution which is fully independent of the 2D polarization state of the generating paraxial source, surviving even for unpolarized light. Remarkably, unlike transverse spin which is a generic property of non-paraxial optical fields, 2D polarization independent optical helicity is solely attributable to non-paraxial optical vortices. Unlike the polarization dependent optical helicity which is responsible for practically all currently known forms of optical activity and chiral light-matter interactions, the present study opens an avenue for the use of unpolarized light in such studies, a remarkable result when placed in the context of classical optics and another exceptional feature of modern nano-optics.

K A F is grateful to the Leverhulme Trust for funding him through a Leverhulme Trust Early Career Fellowship (Grant Number ECF-2019-398) and thanks David L. Andrews for helpful discussions and Garth A. Jones for help with the figure.

Appendix: spin angular momentum density

The dual symmetric spin angular momentum density for time averaged monochromatic fields is [22]

$$\overline{\boldsymbol{s}} = \frac{\varepsilon_0}{4\omega}\operatorname{Im}\left(\boldsymbol{E}^* \times \boldsymbol{E} + c^2 \boldsymbol{B}^* \times \boldsymbol{B}\right) \equiv \overline{\boldsymbol{s}}^E + \overline{\boldsymbol{s}}^B \tag{A14}$$

Using (3) in (A14), the electric transverse spin density (which comes from the cross product of a transverse field component with the longitudinal component) $\overline{\boldsymbol{s}}_\perp^{E(x)}$ for a 2D-*x* polarized 3D LG mode is

$$\overline{\boldsymbol{s}}_\perp^{E(x)} = -\hat{\boldsymbol{y}}\frac{I(r,z)}{c\omega}\frac{1}{k}\operatorname{Re}\gamma\cos\phi. \tag{A15}$$

Inserting the 2D-*y* polarized electric field (7) in (A14) we get its spin density as

$$\overline{\boldsymbol{s}}_\perp^{E(y)} = \hat{\boldsymbol{x}}\frac{I(r,z)}{c\omega}\frac{1}{k}\operatorname{Re}\gamma\sin\phi. \tag{A16}$$

The magnetic spin density contribution for the 2D-*y* polarized magnetic field (5) (which corresponds to the *x* polarized electric field) is

$$\overline{\boldsymbol{s}}_\perp^{B(y)} = \hat{\boldsymbol{x}}\frac{I(r,z)}{c\omega}\frac{1}{k}\operatorname{Re}\gamma\sin\phi \tag{A17}$$

The corresponding magnetic contribution for the 2D-*y* polarized electric field is calculated using (8) as:

$$\overline{\boldsymbol{s}}_\perp^{B(-x)} = -\hat{\boldsymbol{y}}\frac{I(r,z)}{c\omega}\frac{1}{k}\operatorname{Re}\gamma\cos\phi. \tag{A18}$$

Therefore the 2D-unpolarized result for the dual symmetric spin is calculated as:

$$\begin{aligned}\overline{\boldsymbol{s}}_\perp^n &= \frac{\left(\overline{\boldsymbol{s}}_\perp^{E(x)} + \overline{\boldsymbol{s}}_\perp^{B(y)}\right) + \left(\overline{\boldsymbol{s}}_\perp^{E(y)} + \overline{\boldsymbol{s}}_\perp^{B(-x)}\right)}{2} \\ &= \frac{1}{2}\left(-\underbrace{\hat{\boldsymbol{y}}\cos\phi}_{ele} + \underbrace{\hat{\boldsymbol{x}}\sin\phi}_{mag} + \underbrace{\hat{\boldsymbol{x}}\sin\phi}_{ele} - \underbrace{\hat{\boldsymbol{y}}\cos\phi}_{mag}\right)\frac{I(r,z)}{c\omega}\frac{1}{k}\operatorname{Re}\gamma\end{aligned} \tag{A19}$$

This matches the result in [12] for the 2D-unpolarized Gaussian beam, i.e. $\overline{\boldsymbol{s}}_\perp^{E(n)} = \overline{\boldsymbol{s}}_\perp^{M(n)} = \frac{\overline{\boldsymbol{s}}_\perp^{(n)}}{2}$ (of course in the Gaussian case $\ell = 0$). It is important to compare this 2D-unpolarized result to the case of 2D-polarized light. For a 2D-*x* polarized electric field the dual symmetric spin is

$$\bar{\mathbf{s}}_{\perp}^{E(x-pol)} = \bar{\mathbf{s}}_{\perp}^{E(x)} + \bar{\mathbf{s}}_{\perp}^{B(y)} = \left\{ \underbrace{\hat{\mathbf{x}}\sin\phi}_{mag} - \underbrace{\hat{\mathbf{y}}\cos\phi}_{elec} \right\} \frac{I(r,z)}{c\omega}\frac{1}{k}\operatorname{Re}\gamma, \tag{A20}$$

and what we see is that unlike the 2D polarization-independent optical helicity density contribution in the main manuscript which is completely independent of polarization, the transverse spin angular momentum density is largely independent but

$$\bar{\mathbf{s}}_{\perp}(unpolarized) \neq \bar{\mathbf{s}}_{\perp}(polarized). \tag{A21}$$

For example, an electric dipole probe interacting with the transverse spin density of a 2D-unpolarized beam would couple to

$$\bar{\mathbf{s}}_{\perp}^{E(n)} = \frac{1}{2}\left(\underbrace{\hat{\mathbf{x}}\sin\phi}_{ele} - \underbrace{\hat{\mathbf{y}}\cos\phi}_{ele} \right) \frac{I(r,z)}{c\omega}\frac{1}{k}\operatorname{Re}\gamma, \tag{A22}$$

whereas for a 2D-*x* polarized electric field the spin density experienced by the electric dipole is

$$\bar{\mathbf{s}}_{\perp}^{E(x-pol)} = -\underbrace{\hat{\mathbf{y}}\cos\phi}_{elec} \frac{I(r,z)}{c\omega}\frac{1}{k}\operatorname{Re}\gamma\ . \tag{A23}$$

[1] L. Novotny and B. Hecht, *Principles of Nano-Optics* (Cambridge University Press, Cambridge, 2012).

[2] D. L. Andrews, editor , *Photonics: Scientific Foundations, Technology and Application* (John Wiley & Sons, Inc, Hoboken, New Jersey, 2015).

[3] A. Forbes, M. de Oliveira, and M. R. Dennis, *Structured Light*, Nat. Photonics **15**, 253 (2021).

[4] K. Y. Bliokh and F. Nori, *Transverse and Longitudinal Angular Momenta of Light*, Phys. Rep. **592**, 1 (2015).

[5] K. Y. Bliokh, F. J. Rodríguez-Fortuño, F. Nori, and A. V. Zayats, *Spin–Orbit Interactions of Light*, Nat. Photonics **9**, 796 (2015).

[6] M. Neugebauer, J. S. Eismann, T. Bauer, and P. Banzer, *Magnetic and Electric Transverse Spin Density of Spatially Confined Light*, Phys. Rev. X **8**, 021042 (2018).

[7] P. Shi, L. Du, and X. Yuan, *Spin Photonics: From Transverse Spin to Photonic Skyrmions*, Nanophotonics **10**, 3927 (2021).

[8] M. R. Dennis, *Geometric Interpretation of the Three-Dimensional Coherence Matrix for Nonparaxial Polarization*, J. Opt. Pure Appl. Opt. **6**, S26 (2004).

[9] C. J. Sheppard, *Jones and Stokes Parameters for Polarization in Three Dimensions*, Phys. Rev. A **90**, 023809 (2014).
[10] M. A. Alonso, *Geometric Descriptions for the Polarization for Nonparaxial Optical Fields: A Tutorial*, ArXiv Prepr. ArXiv200802720 (2020).
[11] T. Setälä, A. Shevchenko, M. Kaivola, and A. T. Friberg, *Degree of Polarization for Optical near Fields*, Phys. Rev. E **66**, 016615 (2002).
[12] J. S. Eismann, L. H. Nicholls, D. J. Roth, M. A. Alonso, P. Banzer, F. J. Rodríguez-Fortuño, A. V. Zayats, F. Nori, and K. Y. Bliokh, *Transverse Spinning of Unpolarized Light*, Nat. Photonics **15**, 156 (2021).
[13] K. Lindfors, T. Setälä, M. Kaivola, and A. T. Friberg, *Degree of Polarization in Tightly Focused Optical Fields*, JOSA A **22**, 561 (2005).
[14] K. Lindfors, A. Priimagi, T. Setälä, A. Shevchenko, A. T. Friberg, and M. Kaivola, *Local Polarization of Tightly Focused Unpolarized Light*, Nat. Photonics **1**, 228 (2007).
[15] A. Aiello, P. Banzer, M. Neugebauer, and G. Leuchs, *From Transverse Angular Momentum to Photonic Wheels*, Nat. Photonics **9**, 789 (2015).
[16] M. Neugebauer, T. Bauer, A. Aiello, and P. Banzer, *Measuring the Transverse Spin Density of Light*, Phys. Rev. Lett. **114**, 063901 (2015).
[17] A. Aiello and P. Banzer, *The Ubiquitous Photonic Wheel*, J. Opt. **18**, 085605 (2016).
[18] P. Shi, L. Du, C. Li, A. V. Zayats, and X. Yuan, *Transverse Spin Dynamics in Structured Electromagnetic Guided Waves*, Proc. Natl. Acad. Sci. **118**, e2018816118 (2021).
[19] Y. Chen, F. Wang, Z. Dong, Y. Cai, A. Norrman, J. J. Gil, A. T. Friberg, and T. Setälä, *Structure of Transverse Spin in Focused Random Light*, Phys. Rev. A **104**, 013516 (2021).
[20] R. P. Cameron, S. M. Barnett, and A. M. Yao, *Optical Helicity, Optical Spin and Related Quantities in Electromagnetic Theory*, New J. Phys. **14**, 053050 (2012).
[21] S. M. Barnett, R. P. Cameron, and A. M. Yao, *Duplex Symmetry and Its Relation to the Conservation of Optical Helicity*, Phys. Rev. A **86**, 013845 (2012).
[22] K. Y. Bliokh, A. Y. Bekshaev, and F. Nori, *Dual Electromagnetism: Helicity, Spin, Momentum and Angular Momentum*, New J. Phys. **15**, 033026 (2013).
[23] K. Y. Bliokh, J. Dressel, and F. Nori, *Conservation of the Spin and Orbital Angular Momenta in Electromagnetism*, New J. Phys. **16**, 093037 (2014).
[24] L. D. Barron, *Molecular Light Scattering and Optical Activity* (Cambridge University Press, Cambridge, 2009).
[25] Y. Tang and A. E. Cohen, *Optical Chirality and Its Interaction with Matter*, Phys. Rev. Lett. **104**, 163901 (2010).
[26] P. Lodahl, S. Mahmoodian, S. Stobbe, A. Rauschenbeutel, P. Schneeweiss, J. Volz, H. Pichler, and P. Zoller, *Chiral Quantum Optics*, Nature **541**, 473 (2017).
[27] J. T. Collins, C. Kuppe, D. C. Hooper, C. Sibilia, M. Centini, and V. K. Valev, *Chirality and Chiroptical Effects in Metal Nanostructures: Fundamentals and Current Trends*, Adv. Opt. Mater. **5**, 1700182 (2017).
[28] F. Crimin, N. Mackinnon, J. B. Götte, and S. M. Barnett, *Optical Helicity and Chirality: Conservation and Sources*, Appl. Sci. **9**, 828 (2019).
[29] L. V. Poulikakos, J. A. Dionne, and A. García-Etxarri, *Optical Helicity and Optical Chirality in Free Space and in the Presence of Matter*, Symmetry **11**, 1113 (2019).
[30] M. Krupová, J. Kessler, and P. Bouř, *Recent Trends in Chiroptical Spectroscopy: Theory and Applications of Vibrational Circular Dichroism and Raman Optical Activity*, ChemPlusChem **85**, 561 (2020).
[31] L. A. Warning, A. R. Miandashti, L. A. McCarthy, Q. Zhang, C. F. Landes, and S. Link, *Nanophotonic Approaches for Chirality Sensing*, ACS Nano **15**, 15538 (2021).

[32] Y. Shen, X. Wang, Z. Xie, C. Min, X. Fu, Q. Liu, M. Gong, and X. Yuan, *Optical Vortices 30 Years on: OAM Manipulation from Topological Charge to Multiple Singularities*, Light Sci. Appl. **8**, 1 (2019).
[33] K. A. Forbes, D. Green, and G. A. Jones, *Relevance of Longitudinal Fields of Paraxial Optical Vortices*, J. Opt. **23**, 075401 (2021).
[34] K. A. Forbes and G. A. Jones, *Measures of Helicity and Chirality of Optical Vortex Beams*, J. Opt. **23**, 115401 (2021).
[35] S. M. Barnett and R. Zambrini, *Orbital Angular Momentum of Light*, in *Quantum Imaging* (Springer, 2007), pp. 277–311.
[36] G. J. Gbur, *Singular Optics* (CRC Press, Florida, 2016).
[37] S. Nechayev, J. S. Eismann, G. Leuchs, and P. Banzer, *Orbital-to-Spin Angular Momentum Conversion Employing Local Helicity*, Phys. Rev. B **99**, 075155 (2019).
[38] K. Y. Bliokh, A. Y. Bekshaev, and F. Nori, *Extraordinary Momentum and Spin in Evanescent Waves*, Nat. Commun. **5**, 3300 (2014).
[39] S. Nechayev, J. S. Eismann, R. Alaee, E. Karimi, R. W. Boyd, and P. Banzer, *Kelvin's Chirality of Optical Beams*, Phys. Rev. A **103**, L031501 (2021).
[40] K. A. Forbes and D. L. Andrews, *Optical Orbital Angular Momentum: Twisted Light and Chirality*, Opt. Lett. **43**, 435 (2018).
[41] K. A. Forbes and D. L. Andrews, *Orbital Angular Momentum of Twisted Light: Chirality and Optical Activity*, J. Phys. Photonics **3**, 022007 (2021).
[42] P. Woźniak, I. D. Leon, K. Höflich, G. Leuchs, and P. Banzer, *Interaction of Light Carrying Orbital Angular Momentum with a Chiral Dipolar Scatterer,* Optica **6**, 961 (2019).
[43] R. P. Cameron, J. B. Götte, S. M. Barnett, and A. M. Yao, *Chirality and the Angular Momentum of Light*, Philos. Trans. R. Soc. Math. Phys. Eng. Sci. **375**, 20150433 (2017).
[44] K. A. Forbes and G. A. Jones, *Optical Vortex Dichroism in Chiral Particles*, Phys. Rev. A **103**, 053515 (2021).